Optimal design of acoustical sandwich panels with a genetic algorithm

Tongan Wang[1,*], Shan Li[1], Steven R. Nutt[1]

1. University of Southern California, 3651 Watts Way, VHE 602, Los Angeles, CA 90089, United States

Abstract: An optimization study is performed to design a sandwich panel with a balance of acoustical and mechanical properties at minimal weight. An acoustical model based on higher-order sandwich beam theory is used with mechanical analysis of the maximum deflection at the center of the sandwich panel under a concentrated force. First, a parametric study is performed to determine the effects of individual design variables on the sound transmission loss of the sandwich panel. Next, by constraining the acoustical and mechanical behavior of the sandwich panel, the area mass density of the sandwich panel is minimized using a genetic algorithm. The sandwich panels are constructed from eight face-sheet and sixteen core materials, with varying thicknesses of the face sheets and the core. The resulting design is a light-weight, mechanically efficient sound insulator with strength and stiffness comparable to sandwich structures commonly used in structural applications.

Key words: Sound transmission loss; Sandwich panel; Genetic algorithm; Higher-order theory

*Corresponding author: Present address: Gulfstream Aerospace Corporation, 500 Gulfstream Road, Savannah, GA 31408, United States. E-mail: tonganw@yahoo.com

1. Introduction

Composite sandwich panels are widely used in various industrial applications because they exhibit extremely high stiffness-to-mass ratios. Unfortunately, the same high stiffness-to-mass ratio that imparts mechanical efficiency also imparts efficient transmission and radiation of acoustic noise,

Please cite this article as: Tongan Wang, Shan Li, Steven R. Nutt, **Optimal design of acoustical sandwich panels with a genetic algorithm**, Applied Acoustics, Volume 70, Issue 3, March 2009, Pages 416-425, ISSN 0003-682X, http://dx.doi.org/10.1016/j.apacoust.2008.06.003.

posing a serious vibro-acoustical problem for a variety of engineering systems in which sandwich structures are used. To address this problem, engineers have attempted to identify optimal designs for sandwich panels that balance mechanical and acoustical properties.

Lang and Dym [1] studied the optimal acoustic design of sandwich structures using their theory of sound transmission through sandwich panels [2]. The objective function of the optimization was the average sound transmission loss over the frequency range 1000–4000 Hz. Four design variables were considered – the Young's modulus of the core, the thicknesses of the core, the Young's modulus of the skin and the thickness of the skin. The material density was determined from the Young's modulus by a linear relationship resulting from curve fitting [3]. The core Poisson's ratio is fixed at a value of 0.35, and that for the skin is 0.30. The total panel surface mass was limited to 0.9 g/cm^2. Using the pattern search method [6], various combinations of design variables were evaluated to improve the sound insulation capacity of sandwich panels. The results indicated two possible approaches for improving the sound insulation of sandwich panels: increasing the total mass of the structure, or constraining the stiffness of the core.

Makris et al. [4] reviewed the single-objective optimization study of acoustic sandwich panels [1], and proposed a more sophisticated optimization technique, as well as a different objective function that was physically more appealing, without the errors identified by Dym and Lang [5]. Three optimization techniques were evaluated in terms of reliability, speed of solution, accuracy of the solution, degree of satisfaction of the constraints, and the suitability for the sound TL case, including the Hooke–Jeeves pattern search method [6], the complex method of Box [7], and the flexible tolerance method [8]. Of these three techniques, the flexible tolerance method was chosen as the optimization technique. The objective function was the maximization of the weighted transmission loss average of the sandwich panel over the frequency range 1000–4000 Hz. Similar design variables were adopted as those in Ref. [1]. The total mass was constrained as 26 kg with standard dimensions of 2 m × 2.4 m. The results showed that the optimum TL was typically found at the value of the core density corresponding to the lowest value within the permissible range of core densities established at the start of the optimization search. Closed-form expressions between TL and the core optimization design variables were found for a set of different skins by curve fitting.

Wennhage [9] analyzed the weight optimization of sandwich panels, taking into account both structural and acoustical requirements. Unlike the previous acoustical optimizations, the sound transmission loss was not the objective function, but was used as an acoustical constraint. The sound transmission loss calculation was based on Nilsson's theoretical model [10], which was developed from a formulation for single-layer structures. Consequently, this method could not predict the dilatational behavior of the sandwich panel. A standard solution for sandwich plates was used to define maximum deflection and stresses as structural constraints. The total mass per unit of area of the sandwich panel was chosen as the objective function, and the design variables were the density of the core, the thickness of the core and the thickness of the face sheets. The Young's modulus and shear modulus of the core were related to the density of the core by empirical equations, and other properties for the face sheets were fixed in the study. An optimization package based on the method of Moving Asymptotes [11] was used to find the set of design variables that minimized the objective function under the constraints. Because this method depends on derivatives, the authors had to use a third-order polynomial to approximate the sound transmission loss near the coincident frequency, thus making the acoustical model less accurate.

A theory of sound transmission through sandwich panels developed in a previous paper [12] is used in the present paper to determine what combinations of design variables could result in a sandwich panel satisfying both the sound insulation and mechanical criteria at minimal weight. The acoustical model accounts for both the antisymmetric (bending) and symmetric (dilatational) motions of the sandwich panel, and is reportedly both accurate and efficient in the calculation of sound transmission loss of sandwich panels. A parametric study is performed first to determine the effects of individual design variables on the sound transmission loss of the sandwich panel. The parametric study is followed by an optimization study, in which the total weight per unit of area is chosen as the objective function, with the weight averaged sound transmission loss as the acoustical constraint, and the maximal deflection at the middle of the panel as the mechanical constraint. The genetic algorithm is utilized as the optimization technique. The design variables consist of the elastic moduli, the densities and the thicknesses of the face sheets and the core materials. In contrast to previous studies, the material properties are selected from a more practical material database as opposed to some range of arbitrary numbers. The thicknesses are bounded with a specified range and discretized by genetic algorithm during optimization. The resolution of the thickness values is dependent on the range and the digit of the chromosome used in the optimization. A numerical example is utilized to illustrate the design process. The present approach can serve as a tool to design weight-optimized sandwich panel with improved acoustic and mechanical properties, constructed from a set of available materials.

2. Acoustical model

The sound transmission loss of sandwich panels has been studied by many researchers since 1959. In their pioneering work, Kurtze and Watters estimated the acoustical behavior of sandwich panels using an equivalent circuit method [13]. This approach and several subsequent formulations [10] and [14] treated the core as an incompressible structure, therefore neglecting the symmetric motion of the sandwich panel. The sound transmission loss of sandwich panels has also been predicted by considering both the symmetric and antisymmetric motion of the sandwich panel [2], [5] and [15]. However, some terms in the dynamical models lack physical explanations. The finite element method has also been applied to the prediction of sound transmission loss of sandwich panels [16], although its application was limited to frequencies below 750 Hz because of vast numbers of nodes at higher frequencies. A detailed review of previous analytical predictions of sound transmission loss of sandwich panels can be found in Ref. [12].

The HSAPT (higher-order sandwich plate theory) has been shown to be both efficient and accurate in the estimation of the dynamical behavior of sandwich panels [17]. Both the antisymmetric and symmetric motions of the sandwich panel are considered. This dynamical model of sandwich panels was employed for the prediction of the sound transmission loss of sandwich panels [12]. Comparisons between the theoretical predictions and experimental data showed good agreement. A similar analysis will be used in the present paper as a theoretical model of transmission loss in sandwich panels with transverse–isotropic face sheets and orthotropic core.

The goal of the present paper is to study the intrinsic sound insulation property of the sandwich panel independent of the effects of external installation conditions, such as clamped or simply-supported boundary conditions. Therefore, the sandwich panel is assumed to be infinitely large to remove the influence of boundary conditions. According to the study by Dym [18], asymmetric sandwich panels (sandwich panels with different skins) exhibit higher transmission loss than symmetric sandwich panels (sandwich panels with identical skins) at the sacrifice of weight. With similar weight, symmetric sandwich panels exhibit higher TL than asymmetric sandwich panels of equivalent weight. Therefore, the two face sheets are assumed to be identical, and the transverse shear stress in the face sheets is neglected. The core of the sandwich panel is assumed to be lightweight and relatively soft, yet strong enough to sustain the shearing of the sandwich panel. The core is modeled as a three-dimensional elastic medium, where the core cross-section does not remain planar, and the thickness of the core may change under loading. The in-plane stresses in the core are ignored because of the large ratio of the stiffnesses of the face sheets to that of the core. By making these assumptions, the displacements in the core can be expressed in terms of the displacement components of the face sheets and the shear stress of the core. Finally, using the Lagrange multipliers method, five equations were derived in terms of the four displacements of the face sheets and the shear stress in the core.

For symmetric sandwich panels, the antisymmetric and symmetric motion of the sandwich panel can be treated independently and the five equations [17] decoupled into a set of three equations which describe the antisymmetric motion of the sandwich panel in terms of the two antisymmetric displacements and shear stress in the core,

$$\begin{aligned} &-\frac{1}{35}b(70\rho d+17\rho_c c)\ddot{u}_a+2Ebdu_{a,xx}+\frac{1}{70}b\rho_c c(3c+17d)\ddot{w}_{a,x} \\ &\quad-\frac{3}{70}(b\rho_c c^2/G_c)\ddot{\tau}+2b\tau=0 \end{aligned} \tag{1}$$

$$\begin{aligned} &-\frac{1}{70}b\rho_c c(3c+17d)\ddot{u}_{a,x}+\frac{1}{420}(840\rho I+2b\rho_c c^3+18b\rho_c dc^2 \\ &\qquad+51b\rho_c d^2 c)\ddot{w}_{a,xx}-2EIw_{a,xxxx}-b(2\rho d+\rho_c c)\ddot{w}_a \\ &\qquad-\frac{1}{420}b\rho_c c^2(9d/G_c+2c/G_c+35c/E_c)\ddot{\tau}_{,x}+b(c+d)\tau_{,x} \\ &\quad=-(p_t+p_b) \end{aligned} \tag{2}$$

$$\frac{1}{70}b\rho_c c^2(-3/G_c + 14/E_c)\ddot{u}_a + 2bu_a + \frac{1}{420}b\rho_c c^2(9d/G_c + 2c/G_c - 42d/E_c - 7c/E_c)\ddot{w}_{a,x} - b(c+d)w_{a,x} + \frac{1}{210}b\rho_c c^3(21/E_cG_c - 1/G_c^2)\ddot{\tau} - (bc^3/12E_c)\tau_{,xx} + bc/G_c\tau = 0 \tag{3}$$

and a set of two equations for the symmetric motion in terms of the symmetric displacement components,

$$b(2\rho d + \rho_c c)\ddot{u}_s - 2Ebdu_{s,xx} - \frac{1}{6}b\rho_c c(c+3d)\ddot{w}_{s,x} = 0 \tag{4}$$

$$-\frac{1}{6}b\rho_c c(c+3d)\ddot{u}_{s,x} + \frac{1}{60}(120\rho I + 15b\rho_c cd^2 + 10b\rho_c c^2 d + 2b\rho_c c^3)\ddot{w}_{s,xx} - \frac{1}{3}b(6\rho d + \rho_c c)\ddot{w}_s - (4E_c b/c)w_s - 2EIw_{s,xxxx} = p_b - p_t \tag{5}$$

where u_s, w_s and u_a, w_a are the symmetric and antisymmetric displacement components of the face sheets, respectively; τ is the shear stress in the core; EA and EI are the axial and flexural rigidities of the face sheets, respectively; A and I are the cross sectional area and second moment of inertia of the face sheet, respectively; $()_{,x}$and ($\ddot{}$) denote the derivative with respect to the spatial coordinate x and the second derivative with respect to time, respectively; b is the width of the beam; c is the height of the core; d is the thickness of the face sheet; E_c, G_c are the elastic and shear moduli of the core, respectively; ρ is the material density of the face sheet; ρ_c is the material density of the core; $pi(x, t)$ is the sound pressure acting on the face sheet; and t is the time coordinate. The geometry and external load of the sandwich panel is illustrated inFig. 1, and the transformation between the general motion of the sandwich panel to the antisymmetric and symmetric motions are shown in Fig. 2.

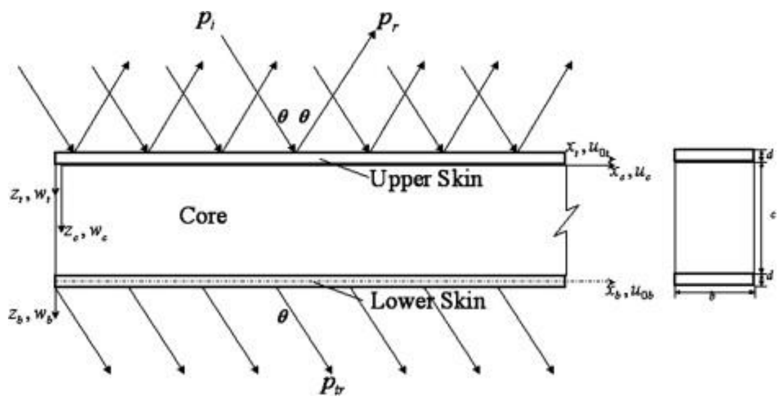

Fig. 1. *Geometry and external loading of the sandwich panel.*

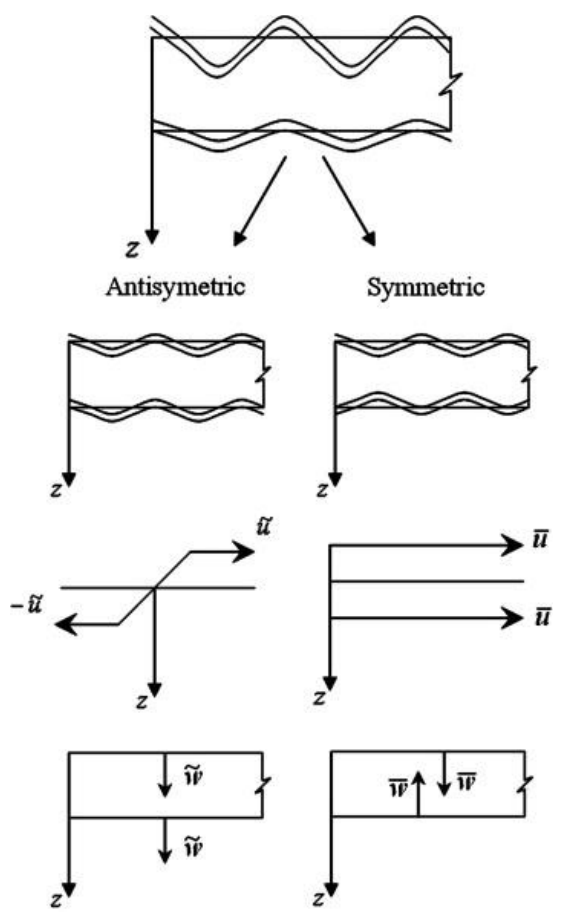

Fig. 2*. Transformation of the general motion of the sandwich panel to antisymmetrid and symmetric motions.*

By substituting the traveling wave form of the displacements and the external pressures, the differential equations were transformed into algebraic equations. The amplitudes of the vertical displacements were solved from the equations, from which the impedances of the antisymmetric and symmetric motions of the sandwich panel were derived by dividing the external pressures by the corresponding velocities (for more details, see Ref.[12])

$$Z_s = -\frac{P_t + P_b}{\dot{W}_s} = -\frac{P_t + P_b}{i\omega W_s} \tag{6}$$

$$Z_a = -\frac{P_t - P_b}{\dot{W}_a} = -\frac{P_t - P_b}{i\omega W_a} \tag{7}$$

Assuming the acoustic particle velocity normal to the panel surface matches the panel velocity at each point, and the reflected pressure has the same amplitude as the incident pressure, the relationship between the incident pressure and the transmitted pressure were obtained in terms of the impedances of the air and the sandwich panel.

$$\tau_{tr} = \left|\frac{p_{tr}}{p_i}\right|^2 = \left|\frac{Z_a/2Z_{air} - Z_s/2Z_{air}}{(1 + Z_a/2Z_{air})(1 + Z_s/2Z_{air})}\right|^2 \tag{8}$$

Damping was incorporated in the calculation through the introduction of complex moduli of the face sheets and the core, where the loss factor was assumed to be frequency independent. This is a sandwich beam theory. However, it also applies for the prediction of sound transmission loss of sandwich panels with isotropic or transverse–isotropic face sheets and core materials. By transforming the stiffnesses of the core by an azmuthal angle ϕ, we also utilized the formulation in the study of sandwich panels with orthotropic core material. Finally, the field incident transmission coefficient was obtained by a numerical integration

$$\bar{\tau}_{\mathrm{tr}} = \frac{\int_{-\pi}^{\pi}\int_{0}^{\theta_0} \tau_{\mathrm{tr}}(\theta,\phi)\sin\theta\cos\theta\,\mathrm{d}\theta\,\mathrm{d}\phi}{\int_{-\pi}^{\pi}\int_{0}^{\theta_0}\sin\theta\cos\theta\,\mathrm{d}\theta\,\mathrm{d}\phi} \tag{9}$$

where $\theta_0 = 78°$ is the empirically determined upper bound of the incident angle [19]. The field-incidence transmission loss was calculated from

$$\mathrm{TL} = 10\log_{10}\left|\frac{1}{\bar{\tau}_{\mathrm{tr}}}\right| \tag{10}$$

The sound transmission losses of four sandwich panels were calculated and the comparisons between the predictions and the experimental data showed good agreement [12]. This analytical tool was utilized in the optimization study to design sandwich panels with transverse–isotropic face sheets and orthotropic core.

3. Parametric Study

3.1 Sound transmission loss of two sandwich panels

Two sandwich panels were used to study the effects of parameters. One is a sandwich panel with polyester fiber glass face sheets and grain balsa wood core; the other is a sandwich panel with isotropic face sheets and honeycomb core. The properties of these two panels are listed in Table 1. First, the HSAPT predictions of these two panels will be compared with the experimental measurements from different labs, and the effects of damping will be studied in the meanwhile. Then, other parameters will be studied in terms of their influence on the STL of sandwich panels. Discussion will be focused on the coincident frequencies of sandwich panels because of their importance in studying STL. Both antisymmetric and symmetric coincident frequencies will be studied.

Table 1. *Material properties of the sandwich panels A and B*

		Thickness (mm)	Elastic modulus (GPa)	Poisson's ratio	Shear modulus (GPa)		Mass density (kg/m^3)
Sandwich panel A	Face sheet	1.524	30	0.33	11.25		1700
	Core	6.75	3.5	–	*Gcxz*	*Gcyz*	144
					0.15	0.15	
Sandwich panel B	Face sheet	6.35	7	0.33	2.6		656.7
	Core	76.2	0.37	–	*Gcxz*	*Gcyz*	28
					0.050	0.023	

Two different setups are widely used to measure the sound transmission loss – one featuring two reverberation rooms [23], or one featuring a reverberation room and an anechoic room [24]. The testing sample is inserted between the two rooms by clamping. Sound sources are placed in the reverberation room to excite a diffuse sound field. The sound transmission loss of the sample is calculated from the transmitted power to the receiving room, which is determined either from the average sound pressure level and the absorption property of the other reverberation room [23], or from the sound intensity scanning data with a sound intensity probe [24]. Sandwich panel A has a dimension of 1.5 m × 1.5 m, and was tested in accordance with ASTM E2249 [24] in USC's Acoustics Lab, and by ASTM E90 [23] in WAL Co. The experimental data of sandwich B was from Ref. [15].

Sandwich panel A is a sandwich panel with polyester fiberglass face sheets and grain balsa wood core. The comparisons between the theoretical HSAPT predictions and experimental measurements are illustrated in Fig. 3, where the dashed bold curve represents the measurement by WAL Co., the solid bold curve is the measurement from the acoustic lab in USC Composite Center, and the solid, dashed and dotted curves correspond to the HSAPT predictions with 2%, 4% and 6% damping in the structure, respectively.

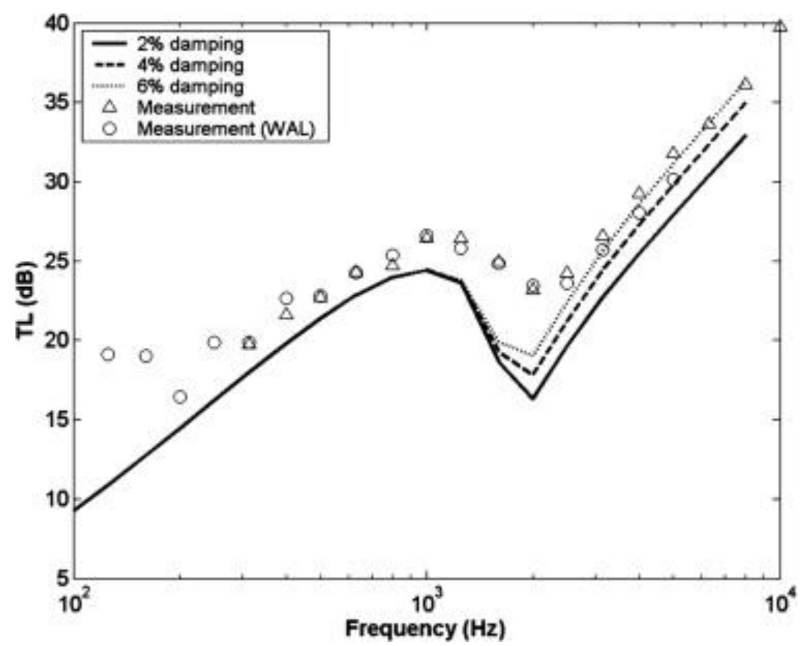

Fig. 3. *Sound transmission loss of sandwich panel with polyester fiberglass faces and grain balsa wood core.*

In Fig. 3, the dip of the STL curve at 1600 Hz corresponds to the antisymmetric coincidence, where the impedance of the antisymmetric motion matches the air impedance. The other symmetric coincidence was not observed in the frequency range of interest (100–8000 Hz) for this sandwich panel, because the balsa wood core is fairly strong and the symmetric coincident frequency was well above 10 kHz. The discrepancies at low frequencies are due to the finite dimension of the test panel. As mentioned in the above, the prediction accounts for the STL of an infinitely large sandwich panel, which is the definite property of a sandwich panel. However, test panels in the measurement always have finite size, which will bring the effect of testing facility and causes low frequencies resonances. In another word, these low-frequency anomalies in the measurements were caused by the testing facility and they will shrink to lower frequency range as we increase the testing panel size and window size. HSAPT was able to predict this antisymmetric coincident frequency and provided consistent trend with the experimental data throughout the frequency range of interest. The dip in the experimental measurements is shallower compared to the HSAPT predictions. This could be partly explained as the influence of damping. As illustrated in Fig. 3, when we increase the damping from 2% to 4% and 6%, the STL increases about 1 dB per step at and after the coincident frequency, while remains the same before the coincident frequency. We applied homogeneous damping value for the whole sandwich panel, which was a rough estimation. More accurate damping model may help improved the accuracy of present HSAPT predictions close to the coincident frequency.

Sandwich panel B has isotropic face sheets and honeycomb core. The comparison between HSAPT prediction and the experimental data [15] shows very good agreement, as shown in Fig. 4. At low frequency, the discrepancies between the experimental data and the theoretical predictions are again attributed to the “finite-panel-size” effect. The low-frequency dip in the predicted TL curve at around 250 Hz corresponds to the antisymmetric coincidence. Experimental trends are consistent with the predictions. In the medium frequency range, the predictions match the experimental data well, and both follow the mass law behavior of sound transmission loss. At 6300 Hz, the experimental data exhibits a dip, which corresponds to the symmetric coincident frequency of the sandwich plate. However, both the present HSAPT prediction and Moore’s prediction hint at this effect at a somewhat higher frequency (around 8000 Hz). The discrepancy at this frequency between the predictions and the measurement is very likely due to an overestimation of the compressive modulus of the core. As shown in Table 1, the compressive modulus of the core was estimated to be 370 MPa. Assuming a reduced modulus of 300 MPa, the dot-dashed curve in Fig. 4 was obtained. This curve closely matches the measured data at 6350 Hz, and retains excellent agreement down to ~500 Hz. The stiffnesses of panel B were estimated from resonance frequency measurements on a test sample consisting of a thin layer of honeycomb sandwiched between rigid metal disks. However, the honeycomb core in sandwich plate B is relatively thick (76 mm), allowing for a greater possibility of modulus-limiting defects. At present, the reason for the apparent reduction of the compressive modulus remains unclear.

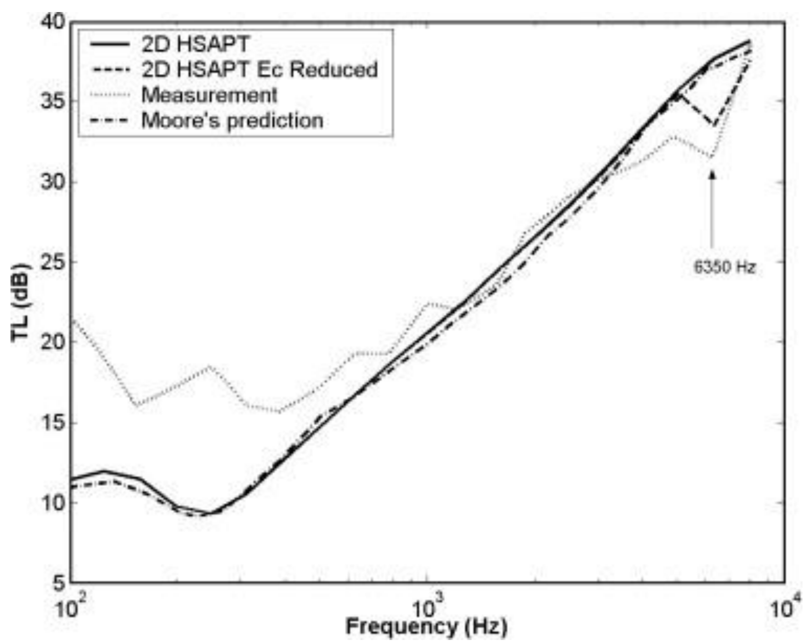

Fig. 4. *Sound transmission loss of sandwich panel with isotropic faces and honeycomb core.*

3.2 Parametric study

Seven properties will be evaluated in this study, including (1) thickness of the face sheet, (2) density of the face sheet, (3) Young's Modulus of the face sheet, (4) density of the core, (5) thickness of the core, (6) compressive modulus of the core, (7) shear modulus of the core. Each property was reduced by 10% at one time, while the other properties remained constant to show its effect clearly. Fig. 5 and Fig. 6 show the influences of these seven parameters on the STL of sandwich panels A and B, respectively, where the *y*-axis represents the change of STL after the parameters are reduced.

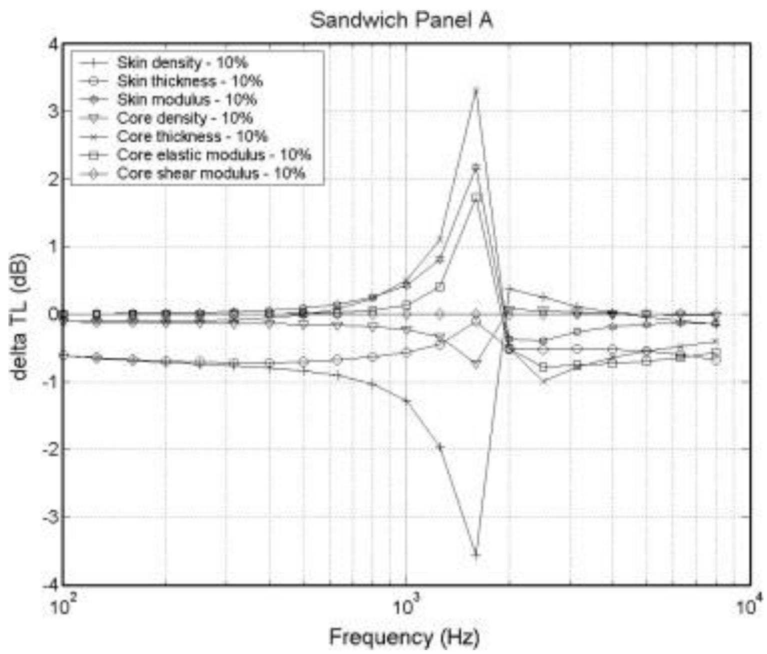

Fig. 5. *Parametric sensitivity comparison chart (−10% variation) as predicted by HSAPT for sandwich panel A.*

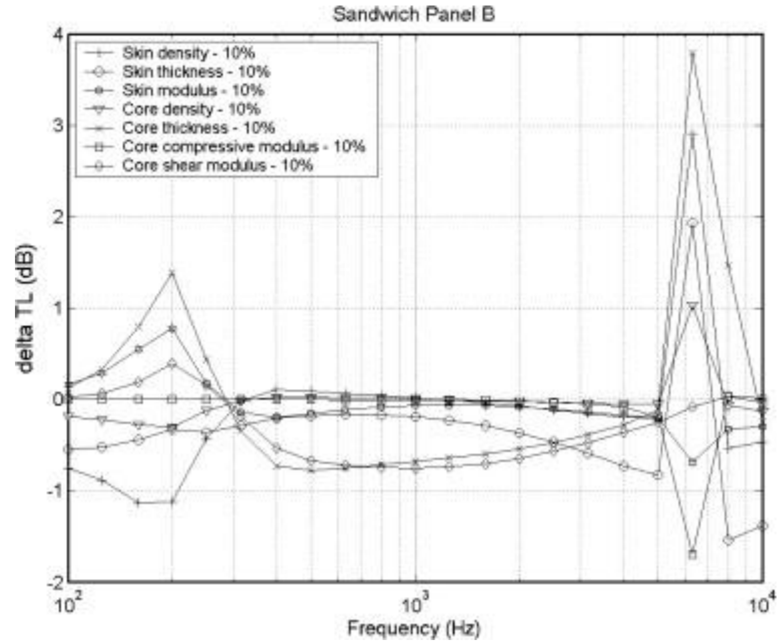

Fig. 6. *Parametric sensitivity comparison chart (−10% variation) as predicted by HSAPT for sandwich panel B.*

3.2.1 Antisymmetric

The sensitivity of the antisymmetric coincident frequency on different parameters will be discussed based on the results for panel A. There are multiple peaks and dips in Fig. 5, which all correspond to the shift of antisymmetric coincident frequencies of sandwich panel A. For example, when the skin density is reduced by 10%, the change of the transmission loss (delta-TL) has a dip followed by a peak. This indicates that the coincident frequency of the panel shifts to lower frequency (at the dip), so the level at the previous coincident frequency (at the peak) is increased. The antisymmetric motion of the sandwich panel can be approximated by pure bending with shearing in the core. There are two key factors in determining the antisymmetric coincident frequency. One is structural stiffness and the other is area mass density. All the seven factors tested in the present work influence STL by affecting these two key parameters. Generally speaking, increasing the mass or decreasing the stiffness will increase the antisymmetric coincident frequency of the structure. Another common knowledge about STL is that heavier structure tends to have better sound insulation property.

Modern sandwich structures generally have heavy, stiff and thin face sheets bonded by light and thick foam or honeycomb core. The overall stiffness of the sandwich structure is most determined by the stiffness of the face sheets, thickness of the core, and the shear stiffness of the core, while the structural mass density is most influenced by the mass density of the face sheets.

As shown by the dips in Fig. 5, as the skin density or core density was decreased, the antisymmetric coincident frequency was lowered. This is due to the fact that the overall stiffness remains the same, while the mass density is reduced. On the other hand, when we reduce the skin Young's modulus, core thickness or core shear modulus, the stiffness of the sandwich panel is reduced, while the change in mass is minor. This leads to the increased antisymmetric coincident frequencies for these three cases, which correspond to the peaks at 1600 Hz in Fig. 5. As also shown in Fig. 5, as we reduced the skin thickness, the overall STL was decreased due to the reduction of weight while the antisymmetric coincident frequency almost remained constant. In this case, both the overall stiffness and mass density of the sandwich structure were reduced, which leads to a cancellation of their influences on the antisymmetric coincident frequency. As core compressive modulus affects neither the overall stiffness nor the mass density of the sandwich structure, its influence on STL can be neglected for the antisymmetric motion.

3.2.2 Symmetric

Sandwich panel B will be utilized to show the effects of different parameters on the symmetric coincident frequency of sandwich panels, which correspond to the peaks and dips at around 6350 Hz in Fig. 6.

As shown in Fig. 6, when skin density, skin thickness, core density or core thickness was reduced, the symmetric coincident frequency was increased; while the symmetric coincident frequency decreases with lower skin Young's modulus or core compressive modulus. Similar to the effect of core compressive modulus on antisymmetric coincident frequency, the influence of core shear modulus is negligible for the symmetric critical frequency.

The symmetric motion of the sandwich panel could be approximated by the dilatational motion of a mass–spring–mass system, with the core serving as the elastic medium connecting the two heavier face sheets. In this case, the symmetric coincident frequency will be influence by the compressive stiffness as well as the overall mass of the sandwich structure. The decrease in overall mass or increase in overall stiffness will both lead to increased symmetric coincident frequency, which is consistent with the observations in Fig. 6.

3.3 Summary of parametric study

As discussed in the above, the sound transmission loss of sandwich panels is influenced by many parameters. In general, increasing mass densities will increase the sound transmission loss of sandwich panels due to the Mass Law. The antisymmetric coincident frequency of the sandwich panel is mainly determined by its flexural stiffness, while its symmetric coincident frequency is influenced by the compressive modulus. At the same time, these parameters affect the mechanical behavior of the sandwich panel, which complicates the design problem. Although higher mass provides higher sound transmission loss, it's not a favorable design for certain applications, such as aerospace industries. As a structural material, sandwich panel is famous for its high stiffness to mass ratio. However, this high stiff to mass ratio will also improve the sound radiation of the sandwich panel, thus resulting in less noise insulation property of the sandwich structure. Therefore, the optimal design of a sandwich panel must satisfy multiple constraints. In the following numerical example, these constrains include both acoustical and mechanical properties of the sandwich panel.

4. Genetic algorithm

A large number of optimization algorithms have been proposed for the nonlinear programming solution. While each technique has its own advantages and disadvantages, including various degrees of efficiency, none of them are suitable for all problems. Thus, the choice of a particular algorithm for any situation depends on the specific problem and the user. Some specific algorithms are considered below.

The pattern search method utilized in Ref. [1] did not have high directional flexibility, and convergence to a global optimum was not guaranteed. A second method – the complex method of Box [7] – is a sequential search technique which has proven effective in solving problems with nonlinear objective functions subject to inequality constraints. Compared to the pattern search method, it has high directional flexibility, and the random generation of points may sample the entire feasible region in a few trials. However, when linear constraints are present, or when equality constraints are involved, the complex method of Box is not very effective. A third method – the flexible tolerance method (FTM) [8] – is a constrained random search technique. In FTM, the set of violated equalities and inequalities is combined in one inequality constraint. As the search process continues, the near-feasibility limits are gradually made more restrictive, until in the limit, only feasible x vectors are accepted. This method has all the advantages of the complex method of Box, and overcame the shortcomings.

In the method of moving asymptotes [11], the solution is computed as a sequence of linearized sub-problems, where each sub-problem is obtained through a Taylor series expansion of the objective function and the constraints about the previous design point. Therefore, for this method to be applicable, the gradients of the objective function and constraints with respect to the design variable changes need to be computed. In the absence of analytic expressions for the derivatives of the objective and constraint functions, a module for finite-difference calculation of the gradient must be provided. Normally, this module is generated by perturbing each design variable by an infinitesimal increment, a process known as sensitivity study. The computation cost is extremely high when it involves a large number of design variables. In addition, this method also has a major disadvantage: convergence cannot be guaranteed, and in practical use this fact sometimes leads to unsatisfactory results.

Genetic algorithms (GAs) [20] represent a popular approach to stochastic optimization, especially with respect to the global optimization problem of finding the best solution among multiple local minima. A fundamental difference between GAs and the random search methods is that GAs work with a population of candidate solutions to the problem. Previous algorithms worked with one solution and moved toward the optimum by updating this one estimate. GAs simultaneously consider multiple candidate solutions to the problem of minimizing the objective function and iterate by moving this population of solutions toward a global optimum. GAs have received increasing attention for a wide range of engineering applications because of the versatile capabilities for both continuous and discrete optimization problems. Research has demonstrated that GAs can be robust in identifying global solutions in multimodal design spaces, even when numerous design variables and constraints are employed. Therefore, GAs are particularly well-suited to the present optimization study.

A major drawback of GAs, however, is numerous iterations are required to achieve a global optimum. In particular, conventional GAs employ a relatively large population size (∼100). As a result, the prohibitive computational cost of carrying out the required function evaluations renders them impractical for high-fidelity models. Some researchers have recently proposed a modified GA called micro-GA [21], in which the population size is 5–7. By doing so, the search efficiency is greatly improved in problems involving a large number of candidates. The micro-GA method will be utilized in the present study.

4.1 Objective function/fitness function

Mass is an important design parameter in aerospace applications. It affects almost all design aspects, including required engine thrust, wing design, and the cost of the aircraft. For this reason, the total mass per unit of area of the sandwich panel was chosen as the objective function. It can be calculated from the mass densities and the thicknesses of the face sheets and the core materials.

$$W=2\rho_{skin}t_{skin}+\rho_{core}t_{core} \tag{11}$$

4.2 Design variables

Seven design variables were selected for the optimization study, including the Young's modulus, the density, the thickness of the face sheets, and the Young's modulus, the shear modulus, and the density and thickness of the core material. Unlike previous optimization studies, the material properties, including the elastic moduli and the densities, were chosen from a limited material database (instead of varying continuously over a range, because practical material properties are discrete instead of continuous values). The damping of the materials was assumed to be independent of frequency, with a fixed loss factor value of 3%.

The face sheets were four alloys and four fiber-reinforced composites. The core was chosen from sixteen materials, including five foams, five honeycombs, a mineral wool, a plywood, a cork, a HDPE and a rubber. The properties of these materials are listed inTable 2 and Table 3. SI units are utilized in the present study. The thickness of the face sheets varied from 0.001 m to 0.01 m, and the thickness of the core lies between 0.01 m and 0.1 m.

Table 2. *Material properties of the face sheet materials*

Materials	Density (kg/m^3)	Young's modulus (GPa)	Shear modulus (GPa)
Steel	7800	210	80
Aluminum	2700	71	26.7
Cast iron	7200	130	52
Titanium	4500	110	41
Graphite/epoxy	1600	125	3.0
Fiberglass/epoxy	1900	56	4.2
Carbon	1600	324	1.1
Aramid/epoxy	1500	76	2.3

Table 3. *Material properties of the core materials*

Materials	Density (kg/m^3)	Young's modulus (MPa)	Shear modulus (MPa)
Polyurethane foam	22	0.0465	0.0166
Melamine foam	8.8	0.08	0.0286
Polyester foam	30	0.54	0.2
Cast foam	22	0.065	0.023
Plastic foam	31	0.143	0.055
Mineral wool	60	6.0	2.0
Hard rubber	1100	2300	772
Honeycomb (1)	48	30	12.5
Honeycomb (2)	24	12	5.0
Balsa wood	144	3500	150
Plywood	700	6.0	2.4
Tricel honey (1)	25.76	9.8	27.5 (L) 11.5 (T)
Tricel honey (2)	38.72	14.6	47.9 (L) 13.0 (T)
Tricel honey (3)	47.2	19.4	63.8 (L) 14.4 (T)
Cork	180	32	5
Polyethylene (HD)	950	1000	0.31e9

4.3 Constraints

Research and experience have demonstrated that designs that favor the mechanical performance of the sandwich panel generally result in high noise transmission and radiation from the panel. To make a sandwich panel more attractive for noise-sensitive applications, both the acoustical the mechanical properties should be constrained.

4.3.1 Acoustical constraint

Makris et. al. [4] utilized an A-weighted sound transmission loss between 1000 Hz and 4000 Hz as the objective function in an optimization study. The same function was employed here to constrain the acoustical behavior of the weight-optimized sandwich panel. The function was determined from a weighted average of the field-incidence transmission coefficients

$$\bar{\tau}_{\mathrm{ave}} = \sum_{i=1}^{7} w_i \bar{\tau}_i \tag{12}$$

in which the weighting function was chosen to correspond to an A-weighting for seven frequencies in the range of 1000–4000 Hz, as given in Table 4.

Table 4. *Normalized weights using the A-weighting [4]*

Frequency (Hz)	A-weighting (dBA)	Normalized weights
1000	0	0.1156
1250	+0.6	0.1327
1600	+1.0	0.1455
2000	+1.2	0.1524
2500	+1.3	0.1559
3150	+1.2	0.1524
4000	+1.0	0.1455
		1.0000

Finally, the weighted sound transmission loss average was calculated from

$$\mathrm{TLA} = -10\lg|\bar{\tau}_{\mathrm{ave}}| \tag{13}$$

Note that larger values of sound transmission loss indicate superior sound insulation. Therefore, the acoustical constraint was defined as

$$\mathrm{TLA} \geqslant \mathrm{TLA}_0 \tag{14}$$

4.3.2 Mechanical constraint

A simple mechanical constraint was employed by considering the maximal deflection of a simply-supported 1 m × 1 m square sandwich plate under 1 N force at the center of the plate. The formula for the deflection at the center of the sandwich plate is [22]

$$d_0 = \frac{\mathrm{PL}^3}{48B_s}(1 + 4k) \tag{15}$$

where B_s is the bending stiffness of the sandwich panel, $k = \frac{3B_s}{A_c G_{eff} L^2}$, G_{eff} is the effective shear modulus of the core. Smaller deflection values indicate greater mechanical stiffness of the sandwich panel. Therefore, the maximal deflection is constrained as

$$\mathrm{d} \leqslant \mathrm{d}_0 \tag{16}$$

Different TLA_0 and d_0 can be chosen for different applications. As an example, TLA_0 = 45 dBA, and d_0 = 0.01 mm are used in the following numerical calculation.

4.4 Optimization strategy

Authors GA's work by maintaining a pool or population of competing designs which are combined to find improved solutions. GA's begin with a set of solutions (represented by chromosomes) called a population. In their basic form, each number of the population is represented by a binary string that encodes the variables characterizing the design. Solutions from one population are taken and used to form a new population. The search progresses by manipulating the strings in the pool to provide new generations of designs, "evolving" to superior properties than their predecessors.

Solutions which are then selected to form new solutions (offspring) are selected according to their fitness – the more suitable they are, the greater chance they have to reproduce. This is repeated until some condition (for example, number of populations or improvement of the best solution) is satisfied. The processes that are used to seek these improved designs are set up to mimic those of natural selection, hence the method's name. The block diagram of GA optimization is illustrated in Fig. 7.

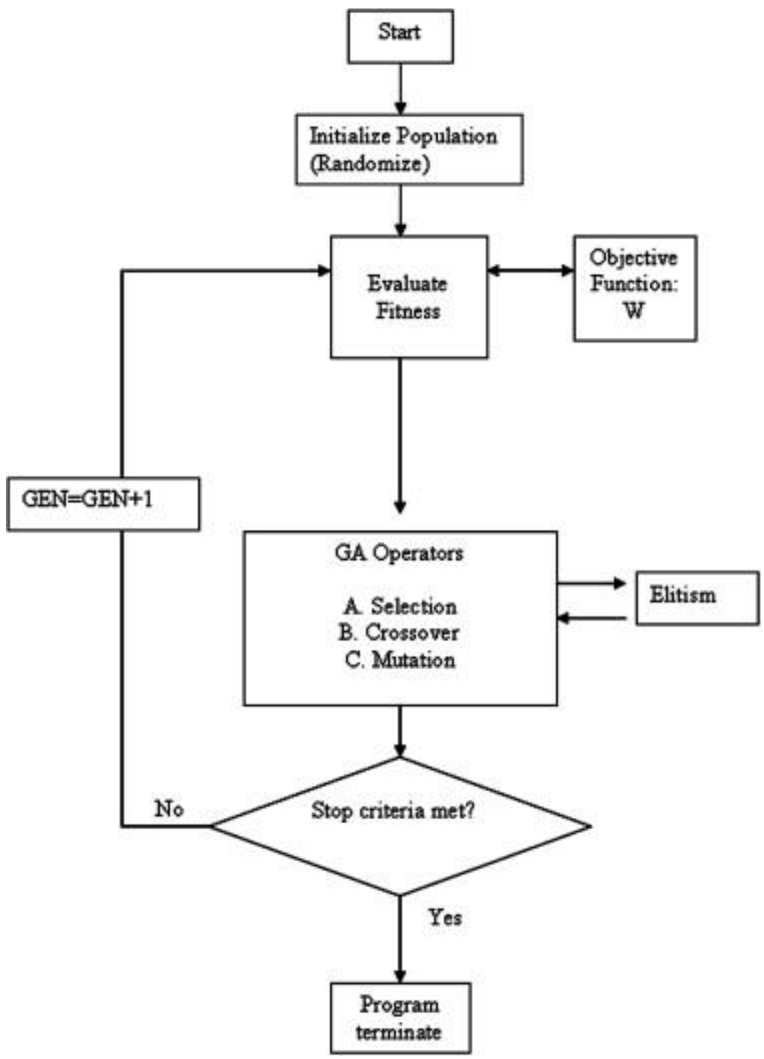

Fig. 7. *Block diagram of GA optimization.*

Both constraints are handled by adopting a simple static penalty method. A constant penalty is applied to those solutions which violate feasibility in any way. The objective function in Eq. (11) is modified as follows:

$$W_{\text{penal}} = W + \sum_i k_i C_i D_i \tag{17}$$

where W_{penal} is the penalized objective function, and *ki* and *Ci* are the *i*th constant penalty coefficient and constraints. The constant *Di* is equal to 1 if *Ci* is violated, and is equal to 0 otherwise. In the present work, different values of the penalty coefficients have been explored. A fixed value of 50 for the penalty coefficients proves to be adequate for the studied penalty function.

4.4.1 Encoding of a chromosome

Design variables are the parameters in a GA optimization. GAs work with a coding of the parameter set, not the parameters themselves. These parameter sets are called chromosomes. Chromosomes should in some way contain information about a solution that it represents. The most common way of encoding is a binary string. Each chromosome is represented by a binary string. Each bit in the string can represent some characteristics of the solution. Another possibility is that the whole string can represent a number.

In the preset optimization, there are 8(=2^3) face sheet materials, 16(=2^4) core materials, and the thicknesses of the face sheet and the core are evenly divided into 512(=2^9) shares. Therefore, a chromosome could look like this:

Chromosome 1	1101100100110110000000111
Chromosome 2	1101111000011110010001001

The first three digits represent the number of the material in the face sheet database, i.e., 000 denotes steel. Similarly, the next four digits are for core materials, such as 1111 might represent Polyethylene. The following nine digits represent the thickness of the face sheet, with 000000000 denoting 1 mm and 111111111 indicating 1 cm. Similarly, the last nine digits represent the thickness of the core.

4.4.2 Genetic operations

The most commonly used operations in GAs are currently: (1) selection according to fitness, i.e., the most promising designs are given a larger share of the next generation; (2) crossover, where portions of two good designs, chosen at random, are used to form a new design, in much the same way that two parents "breed" an "offspring"; (3) mutation, where small but random changes are arbitrarily introduced into a design. In addition, the number of generations and their size must be chosen, as will as a method for dealing with constraints.

(1) Selection

Chromosomes are selected from the population to be parents for crossover. The problem then is how to select these chromosomes. According to Darwin's theory of evolution, the best (or fittest) ones survive to create new offspring. Thus, parents are selected according to their fitness. The more fit the chromosomes, the more chances for selection they have. Imagine a roulette wheel where all the chromosomes in the population are placed. The size of the section in the roulette wheel is proportional to the value of the fitness function of every chromosome – the greater the value, the larger the section.

(2) Crossover

The crossover operator permits the reproduction of new strings through combinations of pairs of strings. A simple crossover operation is done by selecting one crossover point, and one binary string from the beginning of the chromosome to the crossover point is copied from the first parent, while the rest is copied from the second parent

11001011+1101**1111**=**11001111** (18)

For example, in Eq. (16), the crossover point is selected between the forth and the fifth digits of the chromosome. The offspring is reproduced by copying the first four digits of the first parent and the last four digits of the second parent

(3) Mutation

Mutation is the sporadic alteration of chromosomes. Mutation is performed by inverting a bit in the binary code. The position at which the bit is inverted is randomly selected with a small probability.

1**1**001001=>1**0**001001 (19)

In Eq. (17), mutation is performed by inverting the second digit of the chromosome.

(4) Elitism

When creating a new population by crossover and mutation, there is a good chance that we will lose the best chromosome. Elitism is the name for the method that first copies the best chromosome (or few best chromosomes) to the new population. The rest of the population is constructed in the ways described earlier. Elitism can rapidly increase the performance of GA, because it prevents a loss of the best found solution.

5. Results and discussion

A numerical example is provided here to demonstrate the methodology described above. Simply-supported 1 m × 1 m sandwich plates are constructed from the eight face sheets materials and the sixteen core materials. The thickness of the face sheets is allowed to vary from 1 mm to 1 cm, and the range for the thickness of the core is 10 mm to 100 mm. The weight-averaged value of the sound transmission loss at the center frequencies of the 1/3 octave band in the frequency range from 1000 to 4000 Hz is constrained to be greater than 45 dBA. Mechanically, the maximal deflection of the sandwich panel under 1 N force at the center of the plate is required to be less than 0.01 mm based on the simply-supported boundary condition.

Fig. 8 shows the fittest objective function value of each generation, plotted as a function of the generation when using a conventional micro-GA. Five populations are used for each generation. As shown in Fig. 8, the values of the objective function for the best individuals steadily decrease with successive generations, because elitism is employed.

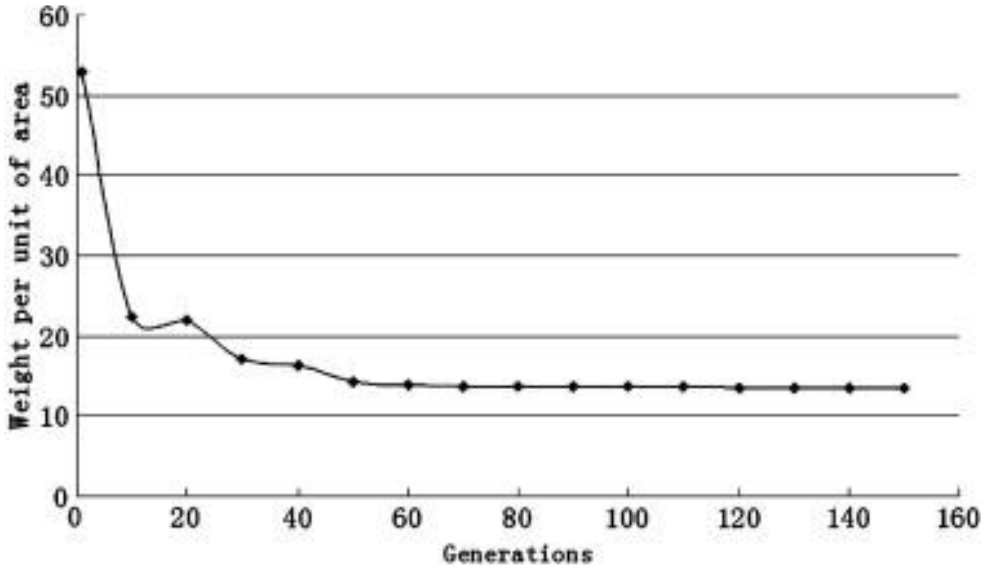

Fig. 8. Variation of the fitness functions with different number of generations.

After 80 generations, the results become stable, and additional generations do not provide more optimal solutions. Finally, we obtain a sandwich panel constructed of titanium face sheets 1.3-mm thick and honeycomb core 72-mm thick with a density of 24 kg/m^2. The results are summarized in Table 5 and the transmission loss curve is shown in Fig. 9.

***Table 5.** Properties of the optimized sandwich panel*

	Mass per unit of area (kg/m^2)	STLA (dBA)	Maximal deflection (mm/N)
Optimized sandwich panel	13.58	45.05	0.007

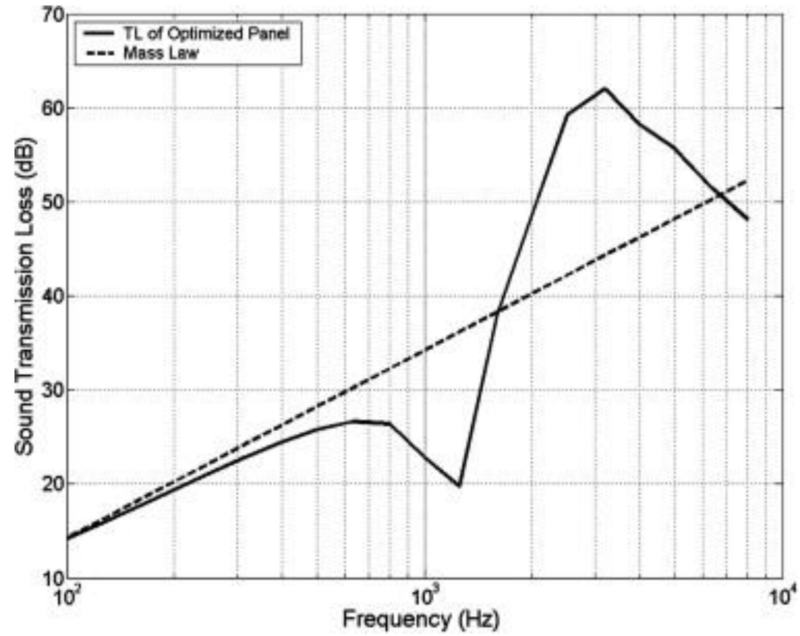

Fig. 9. *Transmission loss of the optimized sandwich panel.*

The transmission loss curve has a dip at 1250 Hz, which corresponds to the symmetric coincident frequency of the optimized sandwich panel. The antisymmetric coincident frequency has been delayed to frequencies higher than the frequency range of interest. Also shown in Fig. 9 is the mass-law transmission loss of an infinite panel with surface mass density equivalent to the optimized sandwich panel (13.58 kg/m^2). The transmission loss of the optimized panel is greater than the mass law at frequencies between the symmetric and antisymmetric coincident frequencies, which is attributed to the "cancellation" of the symmetric and antisymmetric impedances.

The antisymmetric and symmetric impedances of a sandwich panel are a function of incident angle. As an example, Fig. 10 shows the impedance of the optimized sandwich panel with 40° incident angle, which is close to the median of the incident angle range (0°–78°). For other incident angles, the trend of the curves will be similar. At 1250 Hz, the symmetric impedance vanishes, which is consistent with the symmetric coincident dip inFig. 9. Also, the antisymmetric impedance will not vanish in the frequency range of interest, as shown in Fig. 9. Between the two coincidences, the symmetric and antisymmetric impedances are close to each other. According to Eq. (8), when the symmetric and antisymmetric impedances are alike, $\tau_{tr} \rightarrow 0$. Correspondingly, transmission loss will exhibit a local maximum, which explains the high transmission loss values in Fig. 9. Detailed discussion of the impedances' effect on τ_{tr} and transmission loss can be found elsewhere. [12].

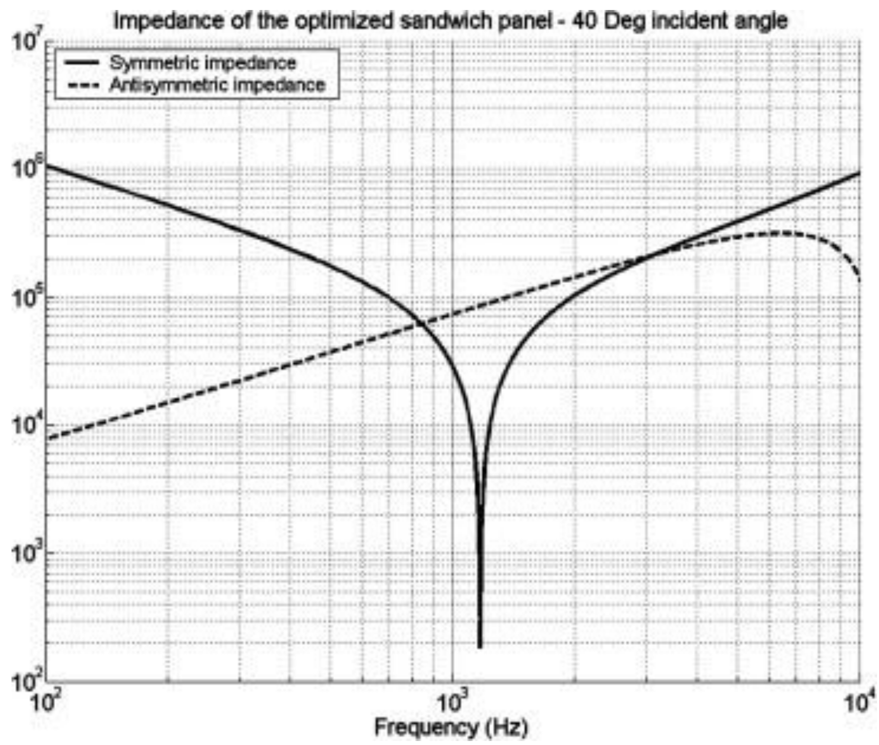

Fig. 10. *Impedance of the optimized sandwich panel with 40° incident angle.*

In the optimized design, the antisymmetric coincidence has been forced outside the frequency range of interest. Although the symmetric coincidence remains in the 1000–4000 Hz range, the cancellation of the two impedances in this range increases the weight-averaged transmission loss significantly. Consequently, the panel exhibits minimal weight while simultaneously satisfying the constraint on transmission loss.

In summary, the total mass per unit area of the sandwich panel is 13.58 kg/m^2, and the weighted sound transmission loss is 45.05 dBA. When 1 N force is applied at the center of the panel, the maximal deflections is 0.007 mm. The sound insulation property constrains the area mass density more than the mechanical property of the sandwich panel, or the mechanical constraint is too loose. Other designs of the sandwich panel can be obtained by changing the constraint values.

6. Conclusions

A sound transmission loss prediction tool based on higher-order sandwich beam theory was used in a parametric study to determine effects of various design variables on the STL of sandwich panels. Subsequently, a weight-optimized sandwich panel was designed using a genetic algorithm, taking into consideration both the acoustical and mechanical properties of the sandwich panel. Eight face sheet materials and sixteen core materials were selected as base materials to design the sandwich panel. The consistent-higher-order prediction was employed to constrain the sound insulation of the sandwich panel, while the maximum deflection of the sandwich panel served as the constraint for the mechanical stiffness.

The mass per unit of area of the sandwich panel was minimized by varying the material properties and thicknesses of the face sheets and core materials, while meeting the acoustical and mechanical constraints for the sandwich panel. The consistent higher-order prediction works compatibly with genetic formulations. The present approach illustrates how the methodologies can serve as practical design tool to optimize sandwich panel designs in terms of both sound insulation and mechanical properties.

Acknowledgements: The authors are grateful to the Merwyn C. Gill Foundation for financial support.

References:

1. Lang MA, Dym CL. Optimal acoustic design of sandwich panels. J Acous Soc Am 1975;57:1481–7.
2. Dym CL, Lang MA. Transmission of sound through sandwich panels. J Acous Soc Am 1974;56:1523–32.
3. Krokosky EM. J Struct Div. ASCE 94, No. ST4. 1968;959–81.
4. Makris SE, Dym CL, Smith JM. Transmission loss optimization in acoustic sandwich panels. J Acous Soc Am 1986;79(6):1833–43.
5. Dym CL, Ventres CS, Lang MA. Transmission of sound through sandwich panels: A reconsideration. J Acous Soc Am 1976:364–7.
6. Hooke R, Jeeves TA. Direct search solution of numerical and statistical problems. J Assoc Comput Math 1961;8:212–9.
7. Box MJ. A new method of constrained optimization and a comparison with other methods. Comput J 1965;8:42–52.
8. Himmelblau DM.Appliednonlinearprogramming.NewYork:McGraw-Hill;1972.
9. Wennhage P. Weight minimization of sandwich panels with acoustic and mechanical constraints. J Sandwich Struct Mater 2001;3:21–48.
10. Nilsson AC. Wave propagation in and sound transmission through sandwich plates. J Sound Vib 1990;138:73–94.
11. Svanberg K. The method of moving asymptotes (mma) with some extensions. Optimization of large structural systems, vol. 1. Kluwer; 1993. p. 555–66.
12. Wang T, Sokolinsky V, Rajaram S, Nutt SR. Assessment of sandwich models for the prediction of sound transmission loss in unidirectional sandwich panels. Appl Acoust 2005;66(3):245–62.
13. Kurtze G, Watters BG. New wall design for high transmission loss or high damping. J Acous Soc Am 1959;31:348–739.
14. Narayanan S, Shanbhag RL. Sound transmission through a damped sandwich panel. J Sound Vib 1982;80:315–27.
15. Moore JA, Lyon RH. Sound transmission loss characteristics of sandwich panel constructions. J Acous Soc Am 1991;89:777–91.
16. Papadopoulos CI. Development of an optimized, standard-compliant procedure to calculate sound transmission loss: numerical measurements. Appl Acoust 2003;64:1069–85.
17. Sokolinsky VS, Nutt SR. Consistent higher-order dynamic equations for softcore sandwich beams. AIAA J 2004;42:374–82.
18. Dym CL, Lang MA. Transmission loss of damped asymmetric sandwich panels with orthotropic cores. J Sound Vib 1983;88(3):299–319.
19. Crocker MJ. Noise and noise control. CRC Press; 1975. p. 58..
20. Holland J. Adaptation in natural and artificial systems. MIT Press; 1998.

21 Krishnakumar K. Micro-genetic algorithm for stationary and non-stationary function optimization, SPIE 1196. Intell Contr Adapt Syst 1989:289–96.

22. Davies JM. Lightweight sandwich constructions. Oxford: Wiley Blackwell; 2001.

23 ASTM E90. Standard test method for laboratory measurement of airbornesound transmission loss of building partition and elements. United States: ASTM International; August 2002.

24. ASTM E2249. Standard test method for laboratory measurement of airborne transmission loss of building partitions and elements using sound intensity.United States: ASTM International; June 2003.